Vol. 700: 145–159, 2022
https://doi.org/10.3354/meps14189

MARINE ECOLOGY PROGRESS SERIES
Mar Ecol Prog Ser

Published November 10

Demographics and dynamics of the world's largest known population of oceanic manta rays *Mobula birostris* in coastal Ecuador

Kanina Harty[1,2,*], Michel Guerrero[2,3], Anna M. Knochel[1,2], Guy M. W. Stevens[1], Andrea Marshall[4], Katherine Burgess[4], Joshua D. Stewart[1,5]

[1]The Manta Trust, Catemwood House, Norwood Lane, Corscombe, Dorset DT2 0NT, UK
[2]Fundacion Megafauna Marina del Ecuador (Proyecto Mantas Ecuador), Calle F y Calle A, Lote 19 Urb El Eden, Collaqui, Tumbaco, Quito 170902, Ecuador
[3]Galapagos Science Center, Universidad San Francisco de Quito and University of North Carolina at Chapel Hill, San Cristóbal 200101, Galápagos, Ecuador
[4]Marine Megafauna Foundation, 7750 Okeechobee Blvd, Ste 4-3038, West Palm Beach, FL 33411, USA
[5]Marine Mammal Institute, Department of Fisheries, Wildlife and Conservation Sciences, Hatfield Marine Science Center, Oregon State University, Newport, OR 97365, USA

ABSTRACT: Information on the life history and demographics of oceanic manta rays *Mobula birostris* remains scarce. Using photo-ID data, we describe the demographic structure, population size, and possible environmental drivers of the seasonal occurrence of *M. birostris* at Isla de la Plata and Bajo Copé, Ecuador. We identified a total of 2803 individuals from 3322 encounters over a period of 14 yr (2005–2018). The population sampled at these sites was significantly biased towards males (sex ratio 1F:1.67M) and only 12.9% of individuals were resighted. We used mark–resight models to estimate demographic parameters of the population, including superpopulation size, survival probability, entry/recruitment probability, and detection probability. We also evaluated how these parameters were related to environmental predictors, such as El Niño–Southern Oscillation (ENSO), sea surface temperature (SST), and chlorophyll *a* (chl *a*). Mark–resight analyses indicated that SST, chl *a*, time, and sex, but not ENSO, were important predictors of estimated population parameters. Entry probability peaked in 2012, which coincided with the lowest SST and highest chl *a* concentrations. The best-fit mark–resight model estimated a superpopulation size of 22 316 individuals, with annual estimated abundances of 949–7650 females and 5226–9340 males. Localised sampling of this highly mobile species limits the interpretations of mark–resight analyses, but provides lower bounds for total abundance that indicate the population of *M. birostris* in coastal Ecuador and Peru is likely the largest in the world.

KEY WORDS: Population modelling · Mark–resight · Photo-identification · South America

1. INTRODUCTION

The oceanic manta ray *Mobula birostris* is a large, planktivorous, pelagic ray found circumglobally in tropical to temperate oceans (Kashiwagi et al. 2011, Marshall et al. 2020). Although capable of long-distance movements of 100s to >1000 km (Andrzejaczek et al. 2021), most populations appear to be philopatric (Stewart et al. 2016a), with few examples of long-distance dispersal (Andrzejaczek et al. 2021, Knochel et al. 2022). Due to low reproductive rates, late maturation, long lifespans (40 yr, Stevens et al. 2018), and slow individual growth (Couturier et al. 2012, Stewart et al. 2018a, Marshall et al. 2020),

*Corresponding author: kanina@mantatrust.org

Publisher: Inter-Research · www.int-res.com

manta rays are vulnerable to population declines in response to exploitation, even at low rates of targeted or incidental capture (Dulvy et al. 2014). All manta and devil rays (collectively: mobulids) are currently listed in Appendix II of the Convention on International Trade in Endangered Species (CITES), with the aim to control the international trade of mobulid products, especially gill plates that are marketed as a health tonic in some Asian countries (O'Malley et al. 2016). Mobulid rays are also included in Appendices I and II of the Convention on the Conservation of Migratory Species of Wild Animals (CMS 2014) and Annex 1 of the CMS Memorandum of Understanding on the Conservation of Migratory Sharks (CMS 2018), to encourage participating nations to create management programmes to protect these species and prevent population declines. However, despite these international management advances, manta and devil rays remain threatened by targeted fisheries and bycatch globally (Croll et al. 2016, Stewart et al. 2018a, Fernando & Stewart 2021). Recently, *M. birostris* was reassessed from Vulnerable to Endangered on the IUCN Red List of Threatened Species (Marshall et al. 2020), indicating that current conservation efforts and management plans are not adequately protecting this species.

While focused scientific effort has filled many knowledge gaps for mobulid rays over the past decade (Couturier et al. 2012, Stewart et al. 2018a), information on the life history, population structure, and habitat use of *M. birostris* remains lacking, particularly in the Southeastern Pacific. An almost complete lack of information on abundance prevents informed assessments of how fisheries and other anthropogenic threats are impacting this species. The productive coastal upwelling region focused off Ecuador and Peru is a hotspot for industrial fisheries, many of which incidentally capture mobulids, including *M. birostris* (Croll et al. 2016). Mobulid rays are highly susceptible to incidental capture in a wide variety of fishing gear types, including longlines and purse seine nets (Alfaro-Shigueto et al. 2010, Alfaro-Cordova et al. 2017, Lezama-Ochoa et al. 2019). Post-release mortality rates for mobulids may exceed 57% (Francis & Jones 2016; out of 7 tagged rays that returned data, 4 died within 1-4 d), especially for the larger species, even if they survive the initial capture process (Poisson et al. 2014, Croll et al. 2016). Although the capture of manta or devil rays has been prohibited in Ecuadorian waters since 2010 (Ministerio de Acuacultura y Pesca 2010), bycatch of *M. birostris* has been documented in artisanal fisheries in Peru. Additionally, local artisanal fishermen are known to target devil rays during periods of difficulty when target fish species are scarce (Alfaro-Cordova et al. 2017). Climate change is expected to cause shifts in productivity of the Humboldt Current System (Bertrand et al. 2018), and increased ocean temperatures, deepening stratification, and changes in wind patterns may lead to variable effects on primary production and upwelling strength (Mogollón & Calil 2018, Oyarzún & Brierley 2018). Even though some protection measures are in place, changes to food web dynamics may impact foraging opportunities for manta and devil rays, potentially causing shifts in their distribution and movement patterns that may influence their susceptibility to incidental capture, especially in regional fisheries.

M. birostris tend to be distributed in offshore, pelagic habitats such as seamounts and oceanic islands (Kashiwagi et al. 2011) that are challenging for field researchers to access, resulting in comparatively less scientific attention than their more coastal counterpart, the reef manta ray *M. alfredi* (Stewart et al. 2018a). A handful of more readily accessible coastal aggregation sites of *M. birostris* have supported increased research effort for the species in recent years (Rohner et al. 2013, Stewart et al. 2016a, Beale et al. 2019). In 1996, seasonal aggregations of *M. birostris* were discovered at Isla de la Plata (IDLP), in the Machalilla National Park, and the Bajo Copé Marine Reserve off the coast of Ecuador (M. Guerrero pers. obs.). Research effort at these sites has been ongoing since 2010. The convergence of the equatorial currents, strong upwelling, and the northward-moving Humboldt Current creates the Equatorial Front from June to September, creating a zone of high primary productivity in this region (Flachier et al. 1997, Martínez-Ortiz et al. 2015). Previous research in this area has shown that *M. birostris* may aggregate at IDLP to take advantage of foraging and cleaning opportunities (Burgess 2017), and individuals are known to travel south to northern Peru and west to the Galapagos Islands (Andrzejaczek et al. 2021). The accessibility of IDLP and the large number of *M. birostris* that aggregate during a predictable season each year provides an opportunity to collect robust demographic and individual data that can be used to describe population dynamics and generate estimates of abundance through mark–resight methods.

Mark–resight approaches are widely used in wildlife ecology to generate estimates of species population sizes and trends. Estimates of abundance are essential for evaluating population status and contextualising the potential magnitude of impacts caused

by fisheries and other anthropogenic threats. In the case of *M. birostris*, absolute estimates of abundance are extremely scarce (Beale et al. 2019), and most inferences about population trends in mobulid species more generally are derived from relative indices of abundance, such as sightings or catches per unit effort (Rohner et al. 2013, Ward-Paige et al. 2013, Pacoureau et al. 2021). Photo-identification (photo-ID) has emerged as a reliable method supporting mark–resight studies in manta rays thanks to the unique spot patterns that remain constant across an individual ray's lifetime (Kitchen-Wheeler 2010, Marshall & Pierce 2012). In the present study, photo-ID data was used to describe the demographic structure of the *M. birostris* population at IDLP and Bajo Copé from 2005 to 2018. Here, we explore how environmental factors affect population dynamics using mark–resight analyses and provide estimates of annual abundance and superpopulation size.

2. MATERIALS AND METHODS

2.1. Study sites

All data were collected at dive sites with high sighting rates of *Mobula birostris* around IDLP (1° 16′ 27.1″ S, 81° 4′ 2.6″ W) and Bajo Copé (1° 48′ 7.6″ S, 81° 3′ 8.1″ W) (Fig. 1). *M. birostris* are frequently seen during SCUBA dives at IDLP for approximately 6 wk annually, during August and September (Burgess 2017). The island has shallow rocky reefs (5–15 m) with sandy areas that rapidly descend to 50 m and >100 m north and west of the island, respectively (Fig. 1). Bajo Copé is a seamount located 59 km (37 miles) south of IDLP (Fig. 1). It is a rocky reef interspersed with large sandy patches with depths ranging from 6 to 50 m. This dive site is more exposed than IDLP and drops down to 500 m rapidly to the west (Fig. 1). The small mainland fishing town of Puerto Lopez is 43 km (26 miles) from IDLP, 37 km (23 miles) from Bajo Copé, and is the main departure point for all data collection efforts.

2.2. Data collection and processing

Participants of SCUBA diving trips collected photo-ID data from 2005 to 2018, but there were no data collected or surveys conducted in 2006 and 2008. Contributors of photo-ID images included community scientists (i.e. the public); SCUBA diving instructors and guides (opportunistic sampling); and researchers visiting the sites for dedicated research expeditions. Targeted research trips were conducted from 2010 through 2018. Survey effort was binned into survey days, with a survey day including any SCUBA dives, photo-ID images, or other data collection efforts at either IDLP or Bajo Copé. Annual study periods varied in length each year, and we considered a survey season to begin with the first survey day and end with the last survey day each year, typically extending from early August to mid-September.

Each *M. birostris* has a ventral spot pattern that is unique and remains constant over the animal's lifetime (Marshall & Pierce 2012). Photographs of these spot patterns can be used to identify individuals and record sightings through time and between locations (Marshall & Pierce 2012). Aside from identification purposes, photo-ID images can also be used to document injuries, signs of mating, and maturity status of individuals through time, although these ancillary data are often dependent on image quality and body orientation (Stevens 2016, Stevens et al. 2018).

A sighting was defined as a unique identification of an individual *M. birostris* on a single day. Any subsequent sighting of a *M. birostris* after the day of first identification was regarded as a resighting. Two or more images of an individual *M. birostris* taken on the same day were considered a single sighting. Photographs that were of poor quality or too dark were discarded (Stevick et al. 2001). We evaluated male maturity based on elongation and calcification of the claspers past the pelvic fin margin and the presence of gonad bulges, and divided males into 'adult', 'subadult', and 'juvenile' categories (White et al. 2006, Marshall & Bennett 2010, Stewart et al. 2018b, Strike et al. 2022). Female maturity can be identified by the presence of mating scars on the pectoral fins, participation in courtship behaviour, and evidence of pregnancy (Marshall & Bennett 2010, Stevens 2016). Maturity can also be inferred from visual estimation of body size (Deakos et al. 2011, Couturier et al. 2012). However, both mating scars and disc widths can be hard to determine through ventral photographs of *M. birostris*. Therefore, life-stage determination for females in this study was not conducted.

Photo-ID images were sorted manually, and a database of individuals was created from photo-IDs from 2005 to 2018. A subset of images from 2005 to 2015 were first processed using MantaMatcher (Marshall & Holmberg 2011). The database was manually re-processed along with images from 2016 to 2018, and then a final analysis, using a semi-

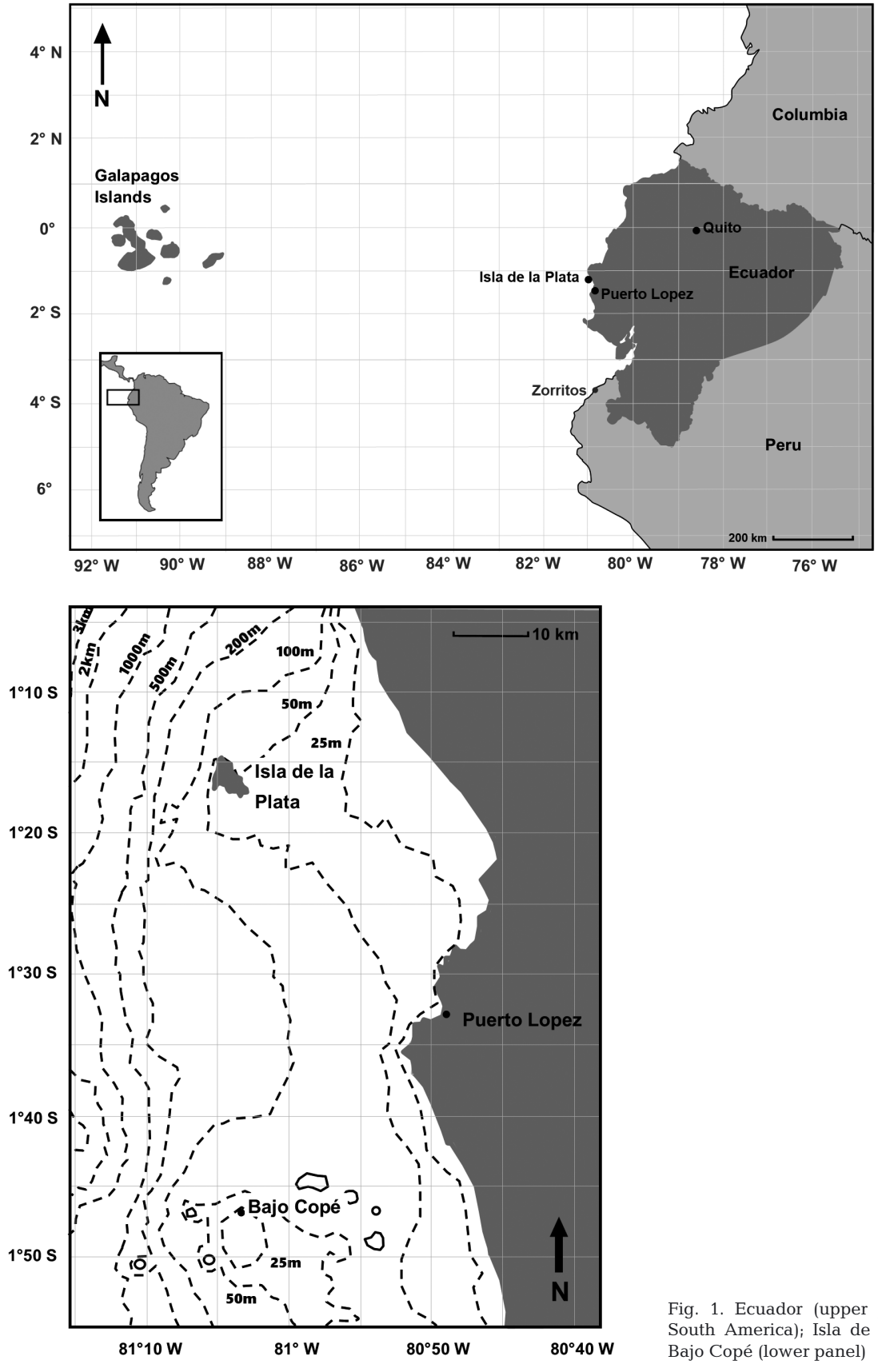

Fig. 1. Ecuador (upper panel; inset: South America); Isla de la Plata and Bajo Copé (lower panel)

automated machine-learning ID matching software, IDtheManta (version: IdTheManta_004_01), was performed to check for duplicates. The database was then compared to existing *M. birostris* photo-ID databases from the Galapagos (n = 169) and Peru (n = 31), using the IDtheManta software to search for matches that may be associated with regional movements.

From the photographs, *M. birostris* were classified into 3 colour morphs (Marshall 2008, Venables et al. 2019). The chevron morph has a distinguishing V-shaped grey band across the posterior ventral surface of the pectoral fins. Leucistic morphs are pale in colour on the dorsal surface and have few or no spots on their ventral side. Melanistic morphs are completely black on their dorsal surface, and most of the ventral surface is also black with limited white patches that are usually present between the gill slits (Stevens et al. 2018). External injuries were recorded, including (1) scars or cuts to the body, pectoral fins, pelvic region and/or claspers; (2) damaged or missing cephalic fins; and (3) observed entanglements with fishing nets and/or lines (Deakos et al. 2011, Strike et al. 2022). Injuries or scars that were more than likely caused by anthropogenic origin, e.g. from fishing lines, nets, or a boat propeller, were noted (Strike et al. 2022). The proportion of males and females in the population was tested with a chi-squared test for significant deviance from a 50:50 sex ratio. We compared the mean number of resightings between males and females using a Kruskal-Wallis test.

2.3. Mark–resight analysis

Mark–resight data were analysed using a POPAN model implemented in R (version 4.1.2) using the RMark package (version 2.2.7) to estimate super-population size, annual abundance, and population parameters Phi (survival probability), p (detection probability), and pent (entry/recruitment probability) (Laake 2013). Given the observed differences in sex ratios in the population, it was hypothesised that sex could be an important factor in detection probability or other parameters estimated in the mark–resight models. Therefore, only individuals with recorded sex were included in the analysis, as the models we used cannot accommodate a combination of known and unknown sex or other variables. As there were only 21 sightings prior to 2009, these sightings were excluded due to minimal, unstructured survey effort in 2005 and 2007, and no effort in 2006 and 2008. Sightings were binned into annual sighting periods, with individual sighting histories indicating presence or absence in each year from 2009 to 2018. *M. birostris* sightings and population dynamics in other regions have been linked to the El Niño–Southern Oscillation (ENSO), sea surface temperature (SST), and chlorophyll *a* (chl *a*) (Beale et al. 2019), so these were considered candidate covariates in the models. Multivariate ENSO indices were obtained from the NOAA Physical Sciences Laboratory and we used the August–September mean values for each year (Wolter & Timlin 2011), as this 2 mo average corresponds to peak *M. birostris* sightings in IDLP and Bajo Copé. The rerddapXtracto R package was used to obtain Aqua MODIS 8 d chl *a* and SST composites at 4 km resolution from a 1° by 1° bounding box centred over IDLP and those data were averaged from 1 August to 30 September in each year. We ran a suite of candidate POPAN models, allowing each model parameter to be constant through time, or to vary by year, by sex, with covariates and with all combinations of these formulations among parameters (Table S1 in the Supplement at www.int-res.com/articles/suppl/m700p145_supp.pdf). The best-fit model was selected using Akaike information criterion values corrected for small sample sizes (AICc).

Open population mark–resight models, such as the POPAN models we used here, make several key assumptions about the data collection process (White & Burnham 1999). These include: (1) all individuals in the population share the same probability of detection; (2) all marked individuals have the same probability of survival; (3) marks are not lost or missed; and (4) sampling is instantaneous relative to the survival interval. Assumptions 2–4 are presumably met in this study, as photo-ID is instantaneous (assumption 4), non-invasive, and therefore should not affect the survival probability of 'marked' individuals (assumption 2), and the spot patterns on manta rays remain constant across their lifetime, so marks cannot be lost (assumption 3). However, the study design almost certainly violates assumption 1. Sampling occurred at primarily 1 site where *M. birostris* aggregate seasonally in large numbers. However, based on satellite tagging studies, the geographic range of this population of *M. birostris* spans the coastlines of southern Ecuador and northern Peru, and 1 individual has been recorded crossing to the Galapagos Islands (Andrzejaczek et al. 2021). Our sampling effort in this study therefore covers only a fraction of the population's geographic range, meaning that individuals that do not visit the IDLP and Bajo Copé aggregation sites have a sighting probability of zero, whereas our models are only able

to estimate demographic parameters for the portion of the population that visits IDLP (or to a lesser extent, Bajo Copé) during the study period. Consequently, estimates of survival probability (Phi) should be interpreted as apparent survival, which is equivalent to (1 − [mortality + emigration out of the study area]), entry probability should be interpreted as the probability that an individual from the population enters the study area for the first time, and estimates of annual abundance should be interpreted as the number of individual *M. birostris* that are present in the study area and available to be sampled. Sampling across the entire geographic range of these highly mobile animals in such a way that would not violate this key assumption is not feasible with current research methods, and therefore correct interpretation of the model-estimated demographic parameters is essential.

3. RESULTS

3.1. Demographic data

A total of 2803 individual *Mobula birostris* were identified from 3322 photo-ID sightings from June 2005 to September 2018 at sites around IDLP and Bajo Copé (Table 1). Most of the total documented sightings (n = 3237; 97.4%) were recorded at IDLP (n = 346 total survey days), while only 2.6% (n = 85) were recorded at Bajo Copé (n = 13 total survey days). All the resighted *M. birostris* recorded in Bajo Copé (n = 7) were initially sighted at IDLP. Most sightings (89%; 2954 out of 3322) were recorded in the months of August and September. The IDthe-Manta matching software found 39 duplicates that were subsequently logged as resightings rather than sightings of new individuals. The recorded photo-IDs were significantly biased towards males (sex ratio 1F:1.67M, χ^2 = 145.88, df = 1, p < 0.0001), with with 1470 males (52%) and 884 females (32%) (Table 2). A majority (83.5%) of the identified males were categorised as mature (n = 1227) based on clasper size within the photo-ID images.

The period from 25 August to 15 September was generally the peak in sightings each year (Fig. 2) and the greatest survey effort was focused during this period to maximise the number of individual *M. birostris* identified each season. While sightings peaked over this period annually, irregular recreational SCUBA dives have observed *M. birostris* as early as April, and as late as December (Fig. 2). The mean number of total sightings per season was 277 ± 216.4. The highest number of individual *M. birostris* sighted in a single day was 60 on 31 August 2018. The number of sightings in a season ranged from a high of 716 in 2012, to a low of 7 in 2005. However, these years also had the highest and lowest number of survey days (n = 55, n = 6) at the dive sites, respectively (Fig. 3). The average number of survey days per season was 32.5 ± 16.2 d (range: 6–55 d).

In terms of colour morphology, 1825 individuals were chevron (65.1%), 524 were leucistic (18.7%), and 454 were melanistic (16.2%) (Table 2). Of the males, 69% (n = 1015) were chevron, 21.6% (n = 317) were leucistic, and 9.4% (n = 138) were melanistic. This was proportionally similar to females, with 71.5% (n = 632) chevron, 19% leucistic (n = 168), and

Table 1. Total number of survey days, sightings, resightings, season period, new individuals, and cumulative total of new individuals, per survey year at Isla de la Plata and Bajo Copé for *Mobula birostris*. Survey effort was not recorded in 2007 and the total number of survey days therefore does not include 2007. na: not applicable/not available

Year	No. of survey days	Sightings	Resightings	Season period	Total no. of new individuals	Cumulative no. of individuals
2005	6	7	0	Jun–Sep	7	7
2007	na	14	0	Unknown	14	21
2009	16	96	2	Aug–Sep	94	115
2010	30	183	13	Jul–Nov	170	285
2011	21	403	41	Aug–Sep	362	647
2012	55	716	95	May–Oct	621	1268
2013	50	311	49	May–Oct	262	1530
2014	48	412	78	Apr–Sep	334	1864
2015	31	142	33	Jun–Sep	109	1973
2016	21	131	29	Apr–Aug	102	2075
2017	48	424	63	May–Sep	361	2436
2018	33	483	116	Jun–Sep	367	2803
Total	359	3322	519	na	2803	na

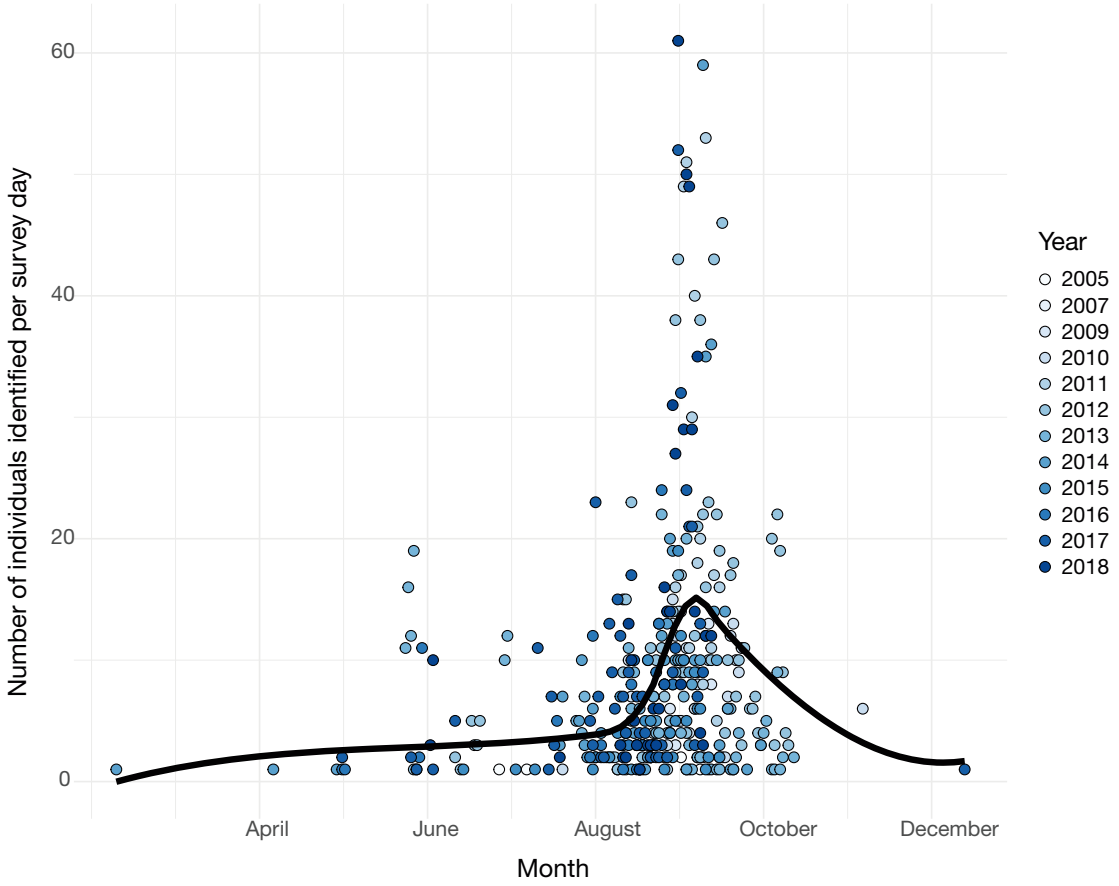

Fig. 2. Survey effort and manta ray sightings. Each point represents 1 d of survey effort; lighter blue represents earlier years, and darker blue, later years. Black line: loess smooth of full data set, indicating average number of sightings per survey day across all years

9.5% (n = 84) melanistic. Of the *M. birostris* of unknown sex, 51.7% (n = 232) were melanistic.

Injury reporting was not standardised throughout the data collection process and injuries were only described for 563 *M. birostris* (out of 2803 recorded individuals). Of those, 71 *M. birostris* were observed entangled in fishing lines, nets, or hooks. Another 277 *M. birostris* had injuries or scars that were likely caused by an anthropogenic source, such as fishing lines, hooks, or nets. Of these, *M. birostris* with damaged or missing cephalic lobes accounted for 64 injuries. Another 113 injuries were likely to have come from natural causes, of which 92 were from infections, remora scarring, or abrasions; and 21 from scarred or injured claspers which likely occurred during mating. Another 102 individuals had injuries for which sources could not be identified. This included animals with scars; missing or damaged tails; bent or broken pectoral fins; damaged pelvic fins or claspers. Lastly, 9 of the identified *M. birostris* observed in this study exhibited wounds associated with shark predation.

Table 2. Recorded population demographic data of oceanic manta rays *Mobula birostris* identified at Isla de la Plata and Baja Copé. M: male; F: female; U: unknown; na: not available

Sex	Individuals	Maturity status				Colour morph type		
		Adult	Subadult	Juvenile	U	Chevron	Leucistic	Melanistic
M	1470 (52%)	1227 (83.5%)	124 (8.4%)	17 (1.2%)	102 (6.9%)	1015 (69%)	317 (21.6%)	138 (9.4%)
F	884 (32%)	na	na	na	884 (100%)	632 (71.5%)	168 (19%)	84 (9.5%)
U	449 (16%)	na	na	na	449 (100%)	178 (39.6%)	39 (8.7%)	232 (51.7%)
Total	2803	1227 (43.8%)	124 (4.4%)	17 (0.6%)	1435 (51.2%)	1825 (65.1%)	524 (18.7%)	454 (16.2%)

Using the IDtheManta software, data from IDLP and Baja Copé were compared to photo-ID databases for the Galapagos Islands (n = 169) and Peru (n = 31). One *M. birostris* (M0042), initially sighted at IDLP on 11 June 2009, was recorded in northern Peruvian waters in June 2015 near oil platforms close to the small town of Zorritos, a straight-line distance of 268 km (Fig. 1). No other regional resightings were recorded.

3.2. Mark–resight analyses

A total of 3322 sightings were recorded from 2005 to 2018. Only 362 *M. birostris* were sighted more than once, resulting in a total resighting rate of 12.9% (362/2803). Over the study period, 158 of the 362 resighted *M. birostris* were sighted in at least 2 different years (158/2803; 5.6% multi-year resighting rate for the population), whereas 204 were resighted only within the same year. The resighting rate was not significantly different between males and females (male: 1.20, female: 1.23, p = 0.82). The maximum time between sightings of an individual was 13 yr: female M0002 was sighted initially on 7 July 2005 and resighted on 27 August 2018.

Mark–resight analysis resulted in 2000 unique combinations of parameter formulations. We list the top 20 model formulations — accounting for 99.99% of the model weight based on AICc values — in Table S1. None of the top 20 models included ENSO as a predictor of any estimated parameter, whereas all top 20 models included SST or chl *a* concentration as a predictor of 1 or more estimated parameters. The top 4 model formulations were within 2 AICc points of the top model and account for 76.3% of the AICc weight (Table 3). SST was included as a predictor of apparent survival (Phi) in 3 of the top 4 models, while chl *a* was included as a predictor of apparent survival in the second-ranked model. Detection probability (p) varied across years in all 4 top models but was generally very low, ranging from 0.01 to 0.06 (Table S2). The top 4 models had extremely similar parameter estimates, except for the second-ranked model, which had slightly lower apparent survival (Phi) estimates in some years than the first-, third-, and fourth-ranked models (Fig. S1). Given the strong agreement among the top 4 models, we only include results from the highest-ranked model in Fig. 4, and in the results and discussion, for simplicity.

The highest-ranked model did not include a sex-specific estimate of the abundance of unobserved individuals (N ~ 1), and therefore the estimate of superpopulation size (which includes both observed and unobserved individuals across the entire study period) was 11 022 (95% CI: 9095–13 357) for females and 11 294 (9456–13 490) for males.

Entry probability was not well estimated in many years, with confidence intervals spanning 0–1, which was a persistent problem across models (Table S2). However, across the top-ranked models, the maximum likelihood estimates for entry probability peaked in 2011 and 2012 (Fig. S1). This large influx of new individuals estimated by the model was followed by low estimated apparent survival in 2012 and 2013 (Fig. 4). In most other years, apparent survival estimates were above 0.9 and entry probability estimates were close to 0 (Figs. 4 & S1, Table S2). Males had higher estimated apparent survival probabilities and lower entry probabilities than females. Apparent survival for both males and females decreased following years with low SST (Fig. 4).

Annual abundance estimates from the highest-ranked model ranged from 949 to 7650 for females and from 5226 to 9340 for males at IDLP and Bajo Copé. Male and female annual abundance estimates peaked in 2012, which coincided with the highest mean chl *a* levels and lowest mean SST of the study period (Fig. 4).

4. DISCUSSION

With 2803 identified individuals and an estimated total abundance of >22 000, the population of *Mobula birostris* seasonally visiting IDLP and Bajo Copé is the

Table 3. The top 4 mark–resight model formulations selected by Akaike information criterion corrected for small sample sizes (AICc). ΔAICc: difference in AICc from the top model; AICc weight: the portion of the overall likelihood received by each model in the full suite of candidate model formulations; Phi: apparent survival; p: detection probability; pent: entry probability; N: superpopulation size

Model formula	AICc	ΔAICc	AICc weight	Deviance
Phi(~Sex + SST)p(~Sex + time)pent(~Sex + time)N(~1)	1799.298	0	0.303235	–9545.73
Phi(~Sex + Chla)p(~Sex + time)pent(~Sex + time)N(~1)	1799.975	0.6767	0.21619	–9545.06
Phi(~Sex + SST)p(~time)pent(~Sex + time)N(~Sex)	1801.03	1.7321	0.127544	–9544
Phi(~Sex + SST)p(~Sex + time)pent(~Sex + time)N(~Sex)	1801.223	1.924613	0.115839	–9545.85

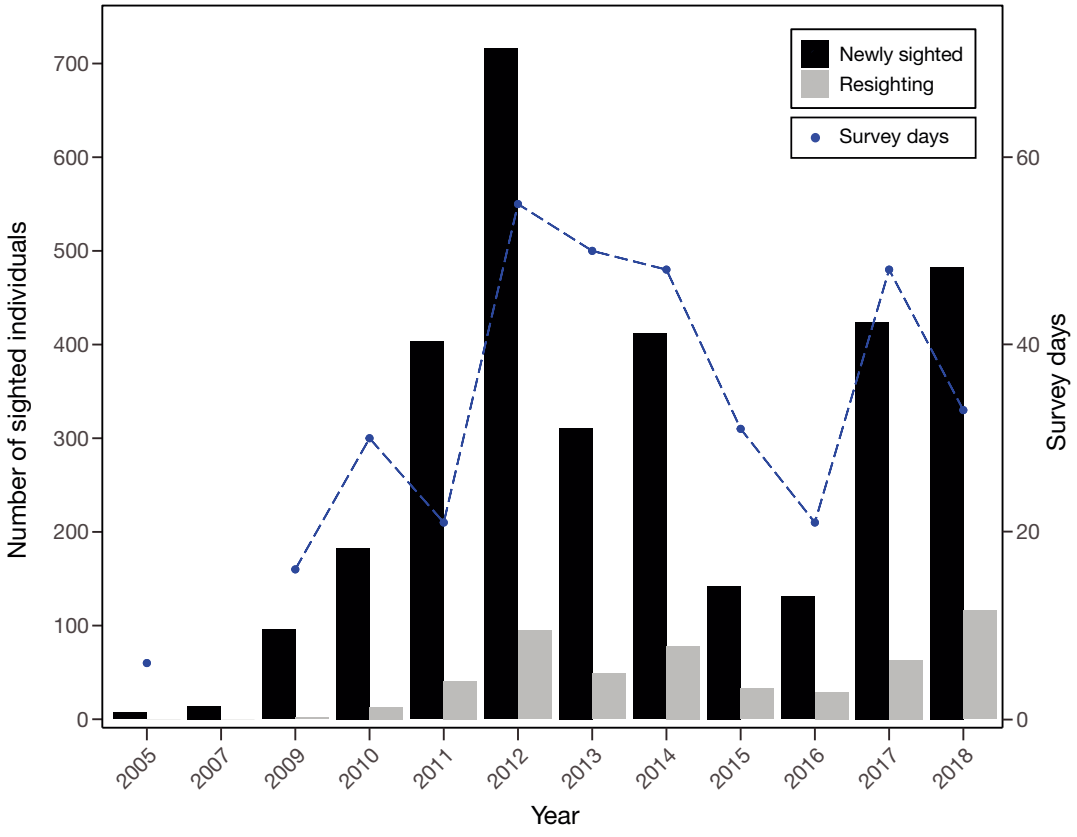

Fig. 3. Total number of *Mobula birostris* sighted (newly sighted and resighted individuals) annually at Isla de la Plata from 2005 to 2018. Sightings represent the first sighting of a newly identified individual; resightings are previously sighted individuals. Blue dashed line: number of days surveying Isla de la Plata and Bajo Copé for each year. The number of survey days that occurred in 2007 was not recorded

largest recorded in the world. Current photo-ID databases for *M. birostris* across multiple studied subpopulations rarely exceed 1000 recorded individuals: 267 identified individuals in the Red Sea (Knochel et al. 2022); 588 in Raja Ampat, Indonesia (Beale et al. 2019); 101 in Mozambique (Marshall 2008); 1141 in the Revillagigedo Archipelago, Mexico (K. Kumli pers. comm.); 286 in coastal Mexico (J. D. Stewart unpubl. data); and 678 in the Maldives (Hilbourne & Stevens 2019). The only other total abundance estimates of *M. birostris* populations are 600 in Mozambique (Marshall 2008) and 1875 from Raja Ampat (Beale et al. 2019), an order of magnitude smaller than our estimate for IDLP and Bajo Copé.

The top POPAN mark–resight model indicated an unprecedented superpopulation size of 22 316 individuals. This reflects the low overall resighting rate (12.9%), low multi-year resighting rate (n = 158; 5.6% of identified individuals), and short periods of time spent over days to weeks at IDLP and Bajo Copé, which suggests *M. birostris* are not long-term residents to the immediate area and visit sporadically. This is further reflected in the very low model-estimated detection probabilities of 1–4% each year. Both the number of individuals identified and the superpopulation size estimates in mark–resight models are sensitive to study duration. Longer studies are more likely to include larger numbers of identified individuals, and superpopulation size reflects the total number of individuals both observed and unobserved over the entire study period, meaning that a longer study period is also likely to be associated with a higher superpopulation size estimate. For comparison, Beale et al. (2019) in Raja Ampat, Indonesia had a 6 yr study period (compared to 14 yr in this study, 10 of which were included in the mark–resight analysis), but less than one-fifth as many identified individuals (n = 588) and less than one-tenth of the estimated superpopulation size (n = 1875). In the Revillagigedo Archipelago, Mexico, >40 yr of survey effort has yielded 1141 identified individuals (K. Kumli pers. comm.), and the other study sites noted

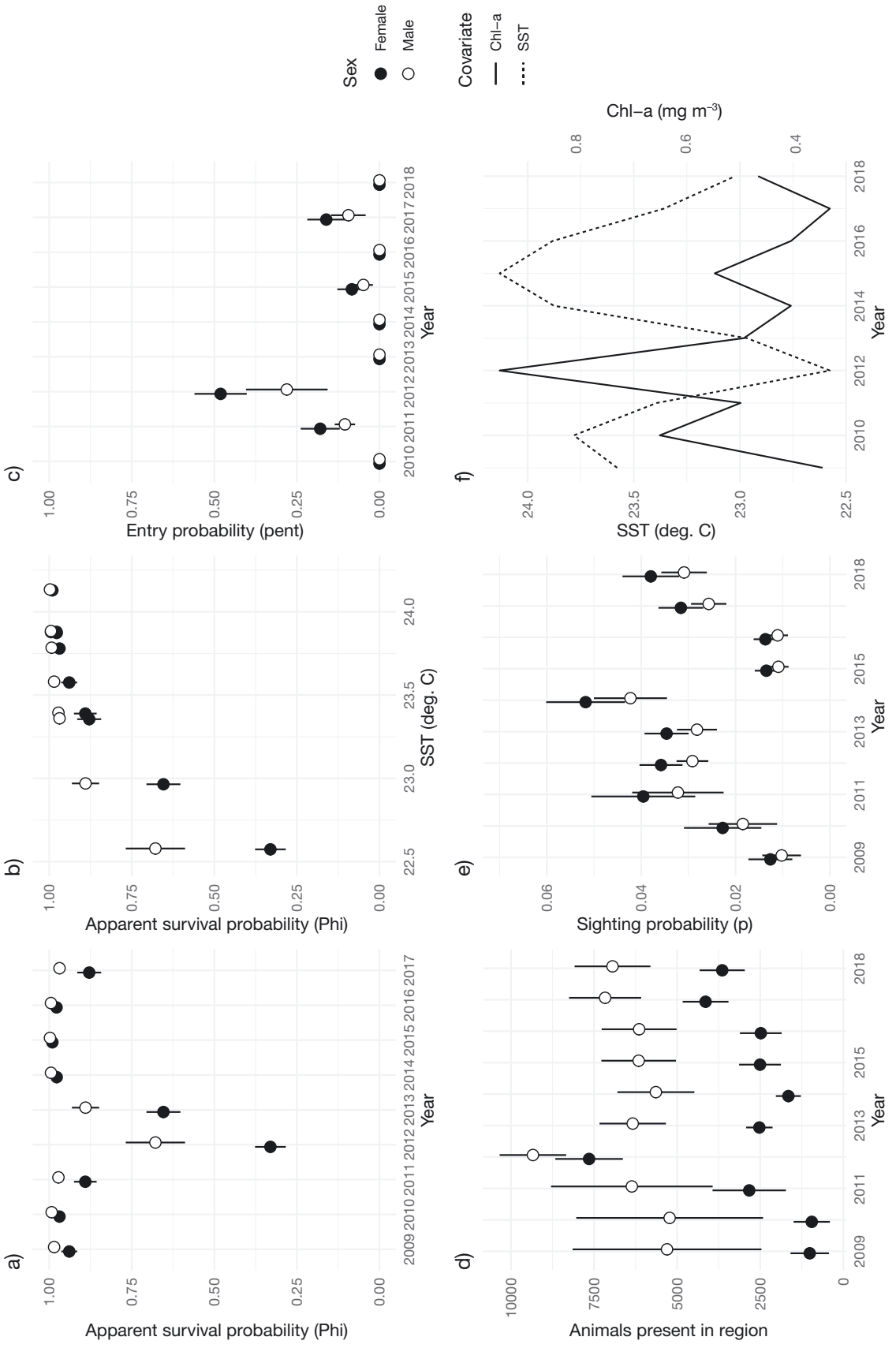

Fig. 4. Top mark–resight model parameter estimates and relationships with environmental covariates. (a) Apparent survival probability for each year from 2009 to 2018. (b) Apparent survival probability plotted relative to sea surface temperature (SST), which was included as a covariate in the top model. (c) Entry probability by year. (d) Regional abundance estimates by year, interpreted as the number of animals present in the study region and available for sampling. (e) Sighting probability by year. (f) SST and chl *a* plotted by year. Error bars: SE of the maximum likelihood estimates

above have identified several hundred individuals over study periods ranging from 5 to 15 yr. In addition, the resighting rate of 12.9% for the IDLP and Bajo Copé population is one of the lowest currently observed of any studied population (Revillagigedo Archipelago: 33.9%, Kumli & Rubin 2008; Raja Ampat, Indonesia: 28%, Beale et al. 2019; Red Sea: 24.3%, Knochel et al. 2022). We therefore conclude that the extremely high estimated abundance for the coastal Ecuador population of *M. birostris* is indeed representative and is not simply a result of study duration. This highlights the potential variability of *M. birostris* population sizes, which may be heavily dependent on regional productivity, and which appear to vary by up to an order of magnitude between regions. This variability has meaningful implications for conservation planning and strategic management development, as the number of individuals that can be lost without causing significant impacts to population viability will be highly dependent on total abundance. Our results highlight the urgent need to generate regional and population-specific abundance estimates for *M. birostris* in order to develop effective management and rebuilding strategies, rather than assuming an average abundance for understudied and unassessed populations.

Contrary to other well studied, female-dominant, *M. alfredi* and *M. birostris* aggregations in Indonesia (Beale et al. 2019), eastern Australia (Couturier et al. 2018), and Mozambique (Marshall 2008), the aggregation observed at IDLP and Bajo Copé is significantly biased towards adult males. Sex-biased segregation or dispersal among elasmobranchs is well documented and can be driven by sexual dimorphism, reproductive needs, or differences in fitness (Phillips et al. 2021). Sex bias in manta ray populations may be reflective of sex segregation in habitat use and the bias in observation effort at these sites rather than a true divergence from a 50:50 sex ratio in the population. For example, in Hawaii, female and male bias is observed in *M. alfredi* at 2 sites located only 15 km apart, further demonstrating that sex bias in habitat use can occur over fine scales (Axworthy et al. 2019). We note that in the present study, despite the observed male-biased sex ratio, our mark–resight models estimated an approximately equal abundance of males and females in the overall population, but sex-specific entry and apparent survival probabilities. The higher apparent survival and higher number of sightings of males that we report here could be indicative of either higher site fidelity to IDLP and Bajo Copé by males, or differing geographic ranges or habitat use in males and females, with our study sites located closer to the activity centre of males than females. In *M. alfredi*, it is hypothesised that higher sightings of females around cleaning stations may be driven by demographic differences in habitat use (Stevens 2016, Nicholson-Jack et al. 2021). Shifts from female to male bias of *M. alfredi* at cleaning stations have been observed during periods of courtship and mating in the Maldives, raising the possibility that these sites could be used as leks (Stevens 2016). We note that sex identification in our study could be influenced by variable detectability of reproductive organs between manta ray color morphs. For example, an outsized proportion of unknown sex individuals (n = 232, 51.7%) were melanistic morphs, which made up only 16.2% (n = 454) of sampled individuals. Water conditions, lighting, orientation of the individual being photographed and color morph may all contribute to bias in the reported sex ratios.

The highest survey effort occurred in 2012 (55 survey days), which coincided with the highest model-estimated regional abundance and the highest number of raw sightings in any year. Although survey effort is not explicitly included in the mark–resighting model, it does account for detection probability, which in this case would most likely be a combination of occupancy rates in the survey area, plus survey effort. As such, the high survey effort in 2012 is not a likely explanation for the high regional abundance estimate in that year, as those effects would be captured in the sighting probability estimates. Further, the following years (2013 and 2014) had similarly high survey effort (50 and 48 survey days), but roughly half as many sightings as 2012. We therefore conclude that the fluctuations in model-estimated regional abundance each year are not reflective of survey effort and are indeed best explained by relationships to the environmental covariates included in the top models (SST and chl *a*).

Apparent survival estimates were low in 2012 and 2013 following high levels of entry in 2011 and 2012. Rather than reflecting true mortality, low survival in these years likely represents emigration away from the study area. A similar pattern of recruitment was observed in Raja Ampat, where lower than expected survival estimates were attributed to this population's use of the Ceram Sea to the southeast of study sites in Raja Ampat (Beale et al. 2019). Based on published satellite tracks of tagged *M. birostris* from Peru and IDLP (Andrzejaczek et al. 2021), the home range of this population appears to be considerably larger than the sampling area covered by our survey efforts, which is a persistent challenge in studies of these mobile, pelagic populations. A low number of sampling sites biases the assumption that resighting prob-

ability is equal across the population and therefore could also contribute to low apparent survival in some years at IDLP and Bajo Copé. A wide variety of factors can influence the migratory movements of large elasmobranchs, such as reproduction, avoidance of predators, or access to foraging opportunities. The *M. birostris* at IDLP and Bajo Copé are largely observed cleaning or cruising and rarely observed feeding (Burgess 2017). However, previous research at this site using isotopic analyses of biopsied muscle samples indicate that a large portion of the diet of *M. birostris* in this population is made up of mesopelagic prey (Burgess 2017). IDLP and Bajo Copé lie close to the edge of the continental shelf and depths of >3000 m would be easily accessible for a large, mobile animal. The proximity to these deep waters and the upwelling created by the Equatorial Front possibly provides ideal foraging conditions that may drive these seasonal aggregations (Scheidat et al. 2000, Martínez-Ortiz et al. 2015, Stewart et al. 2016b, Burgess 2017, Andrzejaczek et al. 2021). *M. birostris* tagged in northern Peru, presumably from the same population as individuals at IDLP and Bajo Copé, demonstrate reverse diel vertical migratory behaviour (Andrzejaczek et al. 2021), meaning that they occupy shallow waters during the day before descending at night, possibly to feed on vertically migrating zooplankton prey. Thus, these sites may act as an aggregation point for *M. birostris* drawn to the region to forage at night where they can also take advantage of cleaning opportunities during the day. Cleaning stations provide opportunities for parasite removal, wound repair, social interactions, and potentially courtship for *M. birostris* (Deakos et al. 2011). It is also hypothesised that both *M. birostris* and *M. alfredi* may utilise cleaning stations or other shallow underwater habitats to thermally recover from cold, deep-water excursions to foraging grounds (Stevens 2016). This kind of behavioural thermoregulation has been observed in sicklefin devil rays *Mobula tarapacana* (Thorrold et al. 2014) and oceanic sunfish *Mola mola* (Nakamura et al. 2015). Further validation of the foraging hypothesis could be facilitated through a combination of satellite tagging, accelerometer measurements, and animal-borne video cameras.

Previous work has suggested that climate systems influence interannual abundance of *M. birostris* (Burgess 2017, Beale et al. 2019). Burgess (2017) suggested that La Niña conditions may increase in the number of *M. birostris* sightings at IDLP and Bajo Copé. However, in contrast to these previous findings, the multivariate ENSO index was not selected in any of the top 20 ranked POPAN models. Rather, the best-fit models included SST or chl *a* as explanatory covariates. ENSO is a major driver of regional SST, upwelling dynamics, and therefore primary productivity in the eastern Pacific, and our results do not rule out ENSO cycles as a major influence on the regional *M. birostris* population. Instead, our results suggest that SST and, to a more limited extent, chl *a* concentrations better predict the observed patterns in apparent survival than the multivariate ENSO index, which summarises a much broader suite of climatic and physical variables that may be less relevant to the movement and population dynamics of this *M. birostris* population. Regional SST and chl *a* were moderately negatively correlated across our study period (correlation coefficient:0.47), and the large number of *M. birostris* observed in 2012 coincided with the highest concentrations of chl *a* and the lowest SSTs in our study period, which may be indicative of a strong period of seasonal upwelling (Dunstan et al. 2018). This suggests, like the conclusions in Burgess (2017), that overall high productivity could be one predictor of *M. birostris* presence at these sites. However, while apparent survival probability was related to SST in the top model, entry probability was not related to any environmental covariates. Aside from the major increase in entry probability in 2012, and subsequent decrease in apparent survival in 2012 and 2013, other years with low SST (e.g. 2018) did not have similarly large increases in entry probability. It is possible that August/September 2012 was an unusually strong upwelling period, as indicated by both the very low SST and high chl *a* values, which reached a productivity threshold and drew an unusually large proportion of the population to the area around IDLP. Further evaluation of secondary productivity (e.g. zooplankton densities) and *M. birostris* visitation to the region is needed to translate the remotely sensed indicators of productivity that we consider here to *in situ* metrics of prey availability and its effect on *M. birostris* visitation to these aggregation sites. Taken collectively with recent studies of *M. birostris* in Indonesia (Beale et al. 2019) and Pacific Mexico (Fonseca-Ponce et al. 2022), our results demonstrate that *M. birostris* habitat use, occupancy, and population dynamics are sensitive to regional-scale oceanographic conditions across a wide variety of habitats and prevailing oceanographic regimes (e.g. eastern versus western boundary currents, temperate rocky versus tropical coral reefs). This has implications for the susceptibility of the species to future climate impacts, as projected decreases in upwelling intensity and primary productivity (Steinacher et al. 2010) could have profound impacts on the species' distribution. This may influence

the probability of interactions with human maritime activities, or the ability of *M. birostris* populations to connect shifting and climate-sensitive foraging grounds with other locations important to their life history, such as reproductive and nursery grounds, that may be geographically limited.

The rate of anthropogenically caused injury to this coastal population of *M. birostris* is difficult to estimate from the data collected in this study. However, of the 563 *M. birostris* that had injuries, more than half (n = 348; 61.8%) were either entangled, or showed evidence of previous line scarring. While the direct targeting of *M. birostris* has been illegal since 2010 in Ecuador, and 2016 in Peru, it is likely that the species still faces threats from fishing activities performed widely throughout the area. Previous satellite tagging revealed that *M. birostris* tagged in Peru spend most of their time within 2 m of the surface during the day (Andrzejaczek et al. 2021). High surface occupation during this time exposes these animals to high risk of entanglement with fishing gear as well as vessel strikes. Future research should address this knowledge gap with comprehensive, standardised injury data collection, to further inform the status of, and threats to, the *M. birostris* population in Ecuador. However, directly estimating the effect of injury status on individual survival probability using mark-resight studies is extremely challenging in highly mobile species when their entire home range is not adequately covered by survey effort. This is compounded when the primary study location is an area with elevated injury risk, for example due to proximity to human population centres. In a study of whale sharks *Rhincodon typus* in the Maldives, sharks that remained within a populated atoll for extended periods had both a higher incidence of anthropogenic injuries, and higher estimated apparent survival in mark-resight models due to their higher residency times. This resulted in mark-resight models estimating a higher survival probability in injured sharks than in uninjured sharks, which spent less time in the study area and therefore had lower injury risk and higher permanent emigration probability (which equates to lower apparent survival probability) (Harvey-Carroll et al. 2021). A similar pattern was found for *M. birostris* near a human population centre in Pacific Mexico (J. D. Stewart et al. unpubl.), highlighting the challenges of quantifying the effects of sublethal human impacts on the survival and population viability of these species. In order to adequately estimate the effect of anthropogenic injuries on *M. birostris* survival probability, future studies will need to either account for the spatial sampling biases present in photo-ID studies of manta rays to estimate absolute survival probability rather than apparent survival probability, or explore alternative methods that are not dependent on survey effort being distributed across the full geographic range of a population.

5. CONCLUSIONS

Our analyses of photo-ID data collected from IDLP and Bajo Copé suggest that the Ecuador *M. birostris* population is the largest known population of the species in the world. This globally significant population currently faces threats from entanglement in fishing gear and is at risk of bycatch in both commercial and artisanal tuna purse seine net, longline, and gillnet fisheries. Male-biased aggregation sites like IDLP and Bajo Copé are uncommon for *M. birostris* and indicates potential sex bias in movements or foraging ecology. The ease of access to these seasonal aggregations of *M. birostris* offer unique opportunities to investigate the species' distribution, habitat use, diving behaviour, and life history. The uncertainty of how the future effects of climate change stand to impact the intensity of upwelling and productivity in the region (García-Reyes et al. 2015) should encourage the continued monitoring of the regional *M. birostris* population to improve our understanding of how these changing oceanographic systems may be influencing the population dynamics and ecology of this endangered species.

Acknowledgements. Very special thanks to Maria Gloria "Yoya" Landazuri for all her dedication, support, invaluable work, and time in the creation and management of the foundation; for all her persistence, patience, dedication, and love for the conservation of manta rays, without her love and help this project would not have been possible. We thank everyone that contributed ID photographs and data, especially Giles 'Stan' Winstanley and Mark Harding. All the team at Exploramar Diving including Luis Lucas Acuña and José 'Cascarita' Quijije; Daniel Lucas, Alejandro Gonzalez and Luis 'Muela' Balón; Jose Solis Carrera, Jorge Antonio Mahuad, Janko Mesec, Juan Manuel Alava, Gustavo Rodriguez, Rafael Espinoza, Eduardo Mahauad, Javier Mahauad, Emiliano Saa, Cristina Carrasco, Fernando Cornejo, Alejandra Rodriguez, Liza Roux and Mike Reich; and Katty Cevallos, Stalin Quijije and Klever Chilan. Thank you Julia Cordero; Jimmy Martinez; Julio Moreno and Oriente Seguros; the crew, staff and volunteers from Machalilla National Park; staff from Subsecretaria de Gestión Marina y Costera del Ecuador, Conservation International, World Wildlife Fund (WWF), Universidad San Francisco de Quito, British Embassy Ecuador, Fernando Emanuele and Orion Energy. Thanks to Save Our Seas Foundation for funding fieldwork and publication. Also funding from Foundation Ensemble, Rufford Foundation, private donors of the Marine

Megafauna Foundation and Ray of Hope Expeditions. A special thanks to Joaquin Guerrero, Joseph Smith Landazuri, Shannon Smith Landazuri and Jonathan Hornby.

Conflict of interest: The authors declare no conflict of interest.

LITERATURE CITED

Alfaro-Cordova E, Del Solara A, Alfaro-Shigueto J, Mangel JC, Diaz B, Carrillo O, Sarmiento D (2017) Captures of manta and devil rays by small-scale gillnet fisheries in northern Peru. Fish Res 195:28–36

Alfaro-Shigueto J, Mangel JC, Pajuelo M, Dutton PH, Seminoff JA, Godley BJ (2010) Where small can have a large impact: structure and characterization of small-scale fisheries in Peru. Fish Res 106:8–17

Andrzejaczek S, Schallert RJ, Forsberg K, Arnoldi NS, Cabanillas-Torpoco M, Purizaca W, Block BA (2021) Reverse diel vertical movements of oceanic manta rays off the northern coast of Peru and implications for conservation. Ecol Solut Evid 2:e12051

Axworthy JB, Smith JM, Wing MS, Quinn TP (2019) Sex biased individual variation in movement patterns of a highly mobile, near-shore marine planktivore, the reef manta ray *Mobula alfredi*. J Fish Biol 95: 1399–1406

Beale CS, Stewart JD, Setyawan E, Sianipar AB, Erdmann MV (2019) Population dynamics of oceanic manta rays (*Mobula birostris*) in the Raja Ampat Archipelago, West Papua, Indonesia, and the impacts of the El Niño–Southern Oscillation on their movement ecology. Divers Distrib 25:1472–1487

Bertrand A, Vögler Santos R, Defeo O (2018) Climate change impacts, vulnerabilities and adaptations: Southwest Atlantic and Southeast Pacific marine fisheries. In: Barange M, Bahri T, Beveridge MCM, Cochrane KL, Funge-Smith S, Poulain F (eds) Impacts of climate change on fisheries and aquaculture: synthesis of current knowledge, adaptation and mitigation options. FAO Fisheries and Aquaculture Technical Paper No. 627. Rome, FAO:325–346

Burgess KB (2017) Feeding ecology and habitat use of the giant manta ray *Manta birostris* at a key aggregation site off mainland Ecuador. PhD thesis, University of Queensland, Brisbane

CMS (Convention on the Conservation of Migratory Species of Wild Animals) (2014) Proceedings of the 11th Meeting of the Conference of the Parties, Quito, Ecuador, 4–9 November 2014. https://www.cms.int/sites/default/files/publication/cms_cop11_proceedings_e.pdf (accessed 18 July 2022)

CMS (2018) Memorandum of Understanding on the Conservation of Migratory Sharks. https://www.cms.int/sharks/en/legalinstrument/sharks-mou (accessed 9 June 2022)

Couturier LIE, Marshall AD, Jaine FRA, Kashiwagi T and others (2012) Biology, ecology and conservation of the Mobulidae. J Fish Biol 80:1075–1119

Couturier LIE, Newman P, Jaine FRA, Bennett MB and others (2018) Variation in occupancy and habitat use of *Mobula alfredi* at a major aggregation site. Mar Ecol Prog Ser 599:125–145

Croll DA, Dewar H, Dulvy NK, Fernando D and others (2016) Vulnerabilities and fisheries impacts: the uncertain future of manta and devil rays. Aquat Conserv 26:562–575

Deakos MH, Baker JD, Bejder L (2011) Characteristics of a manta ray *Manta alfredi* population off Maui, Hawaii, and implications for management. Mar Ecol Prog Ser 429:245–260

Dulvy NK, Pardo SA, Simpfendorfer CA, Carlson JK (2014) Diagnosing the dangerous demography of manta rays using life history theory. PeerJ 2:e400

Dunstan PK, Foster SD, King E, Risbey J and others (2018) Global patterns of change and variation in sea surface temperature and chlorophyll *a*. Sci Rep 8:14624

Fernando D, Stewart JD (2021) High bycatch rates of manta and devil rays in the 'small-scale' artisanal fisheries of Sri Lanka. PeerJ 9:e11994

Flachier A, Sonnenholzner J, Pérez D, Jaramillo L, Espinoza E, EcoCiencia (1997) Evualuación del Área Marina del Parque Nacional Machalilla. Parts 1 and 2. Instituto Ecuatoriano Forestal y de Areas Naturales y Vida Silvestre (INEFAN) and Dirección Nacional de Areas Naturales y Vida Silvestre (DNANVS). Parque Nacional Machalilla, Pto. Lopez (in Spanish)

Fonseca-Ponce IA, Zavala-Jiménez AA, Aburto-Oropeza O, Maldonado-Gasca A, Galván-Magaña F, González-Armas R, Stewart JD (2022) Physical and environmental drivers of oceanic manta ray *Mobula birostris* sightings at an aggregation site in Bahía de Banderas, Mexico. Mar Ecol Prog Ser 694:133–148

Francis MP, Jones EG (2016) Movement, depth distribution and survival of spinetail devilrays (*Mobula japanica*) tagged and released from purse-seine catches in New Zealand. Aquat Conserv 27:219–236

García-Reyes M, Sydeman WJ, Schoeman DS, Rykaczewski RR, Black BA, Smit AJ, Bograd SJ (2015) Under pressure: climate change, upwelling, and eastern boundary upwelling ecosystems. Front Mar Sci 2:109

Harvey-Carroll J, Stewart JD, Carroll D, Mohamed B and others (2021) The impact of injury on apparent survival of whale sharks (*Rhincodon typus*) in South Ari Atoll Marine Protected Area, Maldives. Sci Rep 11:937

Hilbourne S, Stevens G (2019) Maldivian Manta Ray Project oceanic manta ray summary report 2019. The Manta Trust. https://static1.squarespace.com/static/5a196500914e6b09132e911f/t/5d1090a94951180001880a1d/1561366735894/MT_MMRP_Oceanic+Manta+Summary+Report_2019_FINAL.pdf (accessed 18 July 2022)

Kashiwagi T, Marshall AD, Bennett MB, Ovenden JR (2011) Habitat segregation and mosaic sympatry of the two species of manta ray in the Indian and Pacific Oceans: *Manta alfredi* and *M. birostris*. Mar Biodivers Rec 4:e53

Kitchen-Wheeler AM (2010) Visual identification of individual manta ray (*Manta alfredi*) in the Maldives Islands, Western Indian Ocean. Mar Biol Res 6:351–363

Knochel AM, Cochran JEM, Kattan A, Stevens GMW, Bojanowski E, Berumen ML (2022) Crowdsourced data reveal multinational connectivity, population demographics, and possible nursery ground of endangered oceanic manta rays in the Red Sea. Aquat Conserv 32: 1774–1786

Kumli K, Rubin R (2008) Photo-identification of the Manta Ray, *Manta birostris*, in the Revillagigedo Islands, Mexico. Joint Meeting of Ichthyologists and Herpetologists (JMIH) Abstract Book, American Elasmobranch Society Devil Ray Symposium, Montreal, 23–28 Jul 2008. Abstract 0714

Laake JL (2013) RMark: An R interface for analysis of capture-recapture data with MARK. AFSC Processed Rep.

2013-01, Alaska Fish Sci Cent, NOAA, Natl Mar Fish Serv, Seattle, WA. https://apps-afsc.fisheries.noaa.gov/Publications/ProcRpt/PR2013-01.pdf

Lezama-Ochoa N, Hall M, Román M, Vogel N (2019) Spatial and temporal distribution of mobulid ray species in the eastern Pacific Ocean ascertained from observer data from the tropical tuna purse-seine fishery. Environ Biol Fishes 102:1–17

Marshall AD (2008) Biology and population ecology of *Manta birostris* in southern Mozambique. PhD thesis, University of Queensland, Brisbane

Marshall AD, Bennett MB (2010) Reproductive ecology of the reef manta ray *Manta alfredi* in southern Mozambique. J Fish Biol 77:169–190

Marshall AD, Holmberg JA (2011) MantaMatcher photo-identification library. www.mantamatcher.org (accessed 20 June 2021)

Marshall AD, Pierce SJ (2012) The use and abuse of photographic identification in sharks and rays. J Fish Biol 80: 1361–1379

Marshall AD, Barreto R, Carlson J, Fernando D and others (2020) *Mobula birostris*. IUCN Red List Threat Species 2020:e.T198921A68632946 (accessed 7 February 2022)

Martínez-Ortiz J, Aires-da-Silva AM, Lennert-Cody CE, Maunder MN (2015) The Ecuadorian artisanal fishery for large pelagics: species composition and spatio-temporal dynamics. PLOS ONE 10:e0135136

Ministerio de Acuacultura y Pesca (2010) Acuerdo Ministerial Nº 093 (Prohibición de pesca dirigida de mantarrayas). http://acuaculturaypesca.gob.ec/subpesca348-acuerdo-ministerial-n-093-prohibicion-de-pesca-dirigida-de-mantarrayas.html (accessed 1 May 2020)

Mogollón R, Calil PHR (2018) Counterintuitive effects of global warming-induced wind patterns on primary production in the Northern Humboldt Current System. Glob Change Biol 24:3187–3198

Nakamura I, Goto Y, Sato K (2015) Ocean sunfish rewarm at the surface after deep excursions to forage for siphonophores. J Anim Ecol 84:590–603

Nicholson-Jack AE, Harris JL, Ballard K, Turner KME, Stevens GMW (2021) A hitchhiker guide to manta rays: patterns of association between *Mobula alfredi*, *M. birostris*, their symbionts, and other fishes in the Maldives. PLOS ONE 16:e0253704

O'Malley MP, Townsend KA, Hilton P, Heinrichs S, Stewart JD (2016) Characterization of the trade in manta and devil ray gill plates in China and South-east Asia through trader surveys. Aquat Conserv 27:394–413

Oyarzún D, Brierley CM (2018) The future of coastal upwelling in the Humboldt Current from model projections. Clim Dyn 52:599–615

Pacoureau N, Rigby CL, Kyne PM, Sherley RB and others (2021) Half a century of global decline in oceanic sharks and rays. Nature 589:567–571

Phillips NM, Devloo-Delva F, McCall C, Daly-Engel TS (2021) Reviewing the genetic evidence for sex-biased dispersal in elasmobranchs. Rev Fish Biol Fish 31:821–841

Poisson F, Séret B, Vernet AL, Goujon G, Dagorn L (2014) Collaborative research: development of a manual on elasmobranch handling and release best practices in tropical tuna purse-seine fisheries. Mar Policy 44:312–320

Rohner CA, Pierce SJ, Marshall AD, Weeks SJ, Bennett MB, Richardson AJ (2013) Trends in sightings and environmental influences on a coastal aggregation of manta rays and whale sharks. Mar Ecol Prog Ser 482: 153–168

Scheidat M, Castro C, Denkinger J, González J, Adelung D (2000) A breeding area for humpback whales (*Megaptera novaeangliae*) off Ecuador. J Cetacean Res Manag 2:165–171

Steinacher M, Joos F, Frölicher TL, Bopp L and others (2010) Projected 21st century decrease in marine productivity: a multi-model analysis. Biogeosciences 7:979–1005

Stevens G (2016) Conservation and population ecology of manta rays in the Maldives. PhD thesis, University of York. https://etheses.whiterose.ac.uk/16981/1/GuyStevens_Doctoral Thesis_Conservation and Population Ecology of Manta Rays in the Maldives_2016.pdf

Stevens G, Fernando D, Dando M, Notarbartolo di Sciara G (2018) Guide to the manta and devil rays of the world. Wild Nature Press. https://press.princeton.edu/books/paperback/9780995567399/guide-to-the-manta-and-devil-rays-of-the-world

Stevick PT, Palsbøll PJ, Smith TD, Bravington MV, Hammond PS (2001) Errors in identification using natural markings: rates, sources, and effects on capture-recapture estimates of abundance. Can J Fish Aquat Sci 58:1861–1870

Stewart JD, Beale CS, Fernando D, Sianipar AB, Burton RS, Semmens BX, Aburto-Oropeza O (2016a) Spatial ecology and conservation of *Manta birostris* in the Indo-Pacific. Biol Conserv 200:178–183

Stewart JD, Hoyos-Padilla EM, Kumli KR, Rubin RD (2016b) Deep-water feeding and behavioral plasticity in *Manta birostris* revealed by archival tags and submersible observations. Zoology 119:406–413

Stewart JD, Jaine FRA, Armstrong AJ, Armstrong AO and others (2018a) Research priorities to support effective manta and devil ray conservation. Front Mar Sci 5:314

Stewart JD, Nuttall M, Hickerson EL, Johnston MA (2018b) Important juvenile manta ray habitat at Flower Garden Banks National Marine Sanctuary in the northwestern Gulf of Mexico. Mar Biol 165:111

Strike EM, Harris JL, Ballard KL, Hawkins JP, Crockett J, Stevens GMW (2022) Sublethal injuries and physical abnormalities in Maldives manta rays, *Mobula alfredi* and *Mobula birostris*. Front Mar Sci 9:773897

Thorrold SR, Afonso P, Fontes J, Braun CD, Santos RS, Skomal GB, Berumen ML (2014) Extreme diving behaviour in devil rays links surface waters and the deep ocean. Nat Commun 5:4274

Venables SK, Marshall AD, Germanov ES, Perryman RJY and others (2019) It's not all black and white: investigating colour polymorphism in manta rays across Indo-Pacific populations. Proc R Soc B 286:20191879

Ward-Paige CA, Davis B, Worm B (2013) Global population trends and human use patterns of *Manta* and *Mobula* rays. PLOS ONE 8:e74835

White GC, Burnham KP (1999) Program MARK: survival estimation from populations of marked animals. Bird Study 46:S120–S139

White WT, Giles J, Dharmadi, Potter I (2006) Data on the bycatch fishery and reproductive biology of mobulid rays (Myliobatiformes) in Indonesia. Fish Res 82:65–73

Wolter K, Timlin MS (2011) El Niño/Southern Oscillation behaviour since 1871 as diagnosed in an extended multivariate ENSO index. Int J Climatol 31:1074–1087

Editorial responsibility: Simon Pittman, Oxford, UK
Reviewed by: 3 anonymous referees

Submitted: March 8, 2022
Accepted: September 27, 2022
Proofs received from author(s): November 6, 2022